

# 000 001 002 003 004 005 006 007 008 009 010 011 012 013 014 015 016 017 018 019 020 021 022 023 024 025 026 027 028 029 030 031 032 033 034 035 036 037 038 039 040 041 042 043 044 045 046 047 048 049 050 051 052 053 META-TARGET DPO: LEARNING ADAPTIVE CONFIDENCE TARGETS VIA META-LEARNING

Anonymous authors

Paper under double-blind review

## ABSTRACT

Direct Preference Optimization (DPO) offers an effective paradigm for aligning Large Language Models (LLMs), yet its performance can be compromised by noisy or ambiguous preference data common in real-world scenarios. Standard DPO formulations often lack mechanisms to adapt to varying levels of reliability across training instances. This paper introduces Meta-Target DPO (MT-DPO), a novel framework that achieves robust preference alignment by dynamically learning adaptive confidence targets for each preference pair. MT-DPO employs a meta-learning approach where an auxiliary confidence module predicts a sample-specific target probability, representing the degree of belief in the observed preference. This module is informed by intrinsic signals, notably perplexity differentials derived from an anchored reference model, indicative of label consistency. Guided by a small, trusted meta-dataset, the confidence module is trained to generate targets that optimally steer the main policy optimization. MT-DPO optimizes the LLM policy using a cross-entropy objective, effectively minimizing the divergence between the policy’s implied preference probability and the dynamically learned confidence target for each pair. This allows the learning process to naturally down-weight uncertain instances and potentially rectify contributions from mislabeled data by adapting the target across the full confidence spectrum. Comprehensive experiments on standard alignment benchmarks demonstrate that MT-DPO significantly outperforms vanilla DPO and other robust alignment strategies on both clean and synthetically noisy datasets, showcasing its superior adaptability and effectiveness in handling preference uncertainty through learned target modulation.

## 1 INTRODUCTION

The alignment of Large Language Models (LLMs) with human preferences and societal values is a critical prerequisite for their responsible and beneficial application in diverse domains Bai et al. (2022a); Ouyang et al. (2022); Stiennon et al. (2020); Askell et al. (2021). While Reinforcement Learning from Human Feedback (RLHF) Christiano et al. (2017); Ziegler et al. (2019) has been a cornerstone in this endeavor, its operational complexity, training instability Chung et al. (2024); Eisenstein et al. (2023), and sample inefficiency have spurred research into more direct and data-efficient offline alignment techniques Rafailov et al. (2023); Azar et al. (2023); Ethayarajh et al. (2024).

Direct Preference Optimization (DPO) Rafailov et al. (2023) has gained significant traction as a prominent offline method. It reframes the alignment problem by establishing a direct link between the LLM policy and pairwise preference data Eisenstein et al. (2023), thereby obviating the need for explicit reward model training, a core component of traditional RLHF pipelines Ouyang et al. (2022). DPO optimizes the policy to maximize the likelihood of observed preferences under the Bradley-Terry model Bradley & Terry (1952); Hunter (2004). However, a fundamental limitation of the standard DPO formulation is its implicit assumption of clean, deterministic preference labels, where one response is unequivocally superior to another. This ideal often contrasts sharply with the reality of human preference data, which is frequently characterized by inherent ambiguities, varying degrees of rater consensus, or even outright labeling errors due to human biases, task misunderstandings, or annotation inconsistencies Lee et al. (2023); Gao et al. (2024); Chen et al. (2024); Casper et al. (2023). Such imperfections in

054 the training data can severely undermine the robustness of DPO Mitchell (2023), potentially leading  
 055 the LLM to learn skewed or incorrect preference distributions.  
 056

057 Efforts to address these challenges have explored various avenues. Some approaches attempt to in-  
 058 incorporate soft or probabilistic interpretations of preferences. For instance, Geometric-averaged DPO  
 059 (GDPO) Furuta et al. (2024) introduced a mechanism to scale the DPO learning signal based on a  
 060 pre-assigned confidence score, but its original formulation primarily considered scenarios where  
 061 one response was at least as good as the other, thus not fully addressing the spectrum of label noise.  
 062 Other methods focus on robust learning from noisy labels, either by adjusting the loss function based  
 063 on estimated global noise rates Mitchell (2023); Wu et al. (2024) or by developing noise-tolerant ob-  
 064 jectives such as Robust DPO Liang et al. (2024). Data-centric perspectives attempt to identify and  
 065 correct noisy instances Song et al. (2022); Han et al. (2020), with methods like PerpCorrect Kong  
 066 et al. (2024) demonstrating the utility of perplexity differences (PPLDiff) as a signal for detect-  
 067 ing inconsistencies in preference labels using an auxiliary model aligned on a small, clean dataset.  
 068 While these methods offer valuable improvements, they often rely on static heuristics, global noise  
 069 assumptions, or multi-stage pre-processing steps that may not adapt optimally to the fine-grained,  
 070 instance-specific variations in label reliability inherent in real-world preference collections Wu et al.  
 070 (2022).

071 In this work, we propose Meta-Target DPO (MT-DPO), a novel framework that achieves robust  
 072 preference alignment by learning to dynamically generate adaptive confidence targets for each pref-  
 073 erence pair. Instead of relying on fixed or heuristically-derived confidence scores, MT-DPO employs  
 074 a meta-learning strategy Shu et al. (2019); Jiang et al. (2018); Vettoruzzo et al. (2024) to train an aux-  
 075 illiary confidence module. This module predicts a sample-specific target probability  $\hat{p}_n$ , representing  
 076 the model’s dynamically inferred belief in the correctness or strength of the observed preference  
 077 ( $y_1 \succ y_2$ ). Crucially, this confidence module is informed by intrinsic signals indicative of label  
 078 quality, with a particular focus on PPLDiff computed using an anchored reference model Kong et al.  
 079 (2024). The module’s parameters are optimized via a meta-objective defined on a small, trusted  
 080 set of high-quality preference examples ( $\mathcal{D}_{meta}$ ). The LLM policy in MT-DPO is then optimized  
 081 using a cross-entropy objective, aiming to align its implied preference probability (derived from  
 082 the DPO log-ratio) with this dynamically learned target  $\hat{p}_n$ . This adaptive target mechanism allows  
 083 MT-DPO to act akin to standard DPO for high-confidence, correct pairs (where learned  $\hat{p}_n \approx 1$ ),  
 084 naturally down-weight ambiguous instances ( $\hat{p}_n \approx 0.5$ ), and effectively rectify the learning signal  
 085 for likely mislabeled pairs by learning targets approaching zero, thereby navigating the full spectrum  
 085 of preference confidence and label quality.

086 Our main contributions are summarized as follows:  
 087

- We introduce MT-DPO, a novel meta-learning framework for robust preference optimiza-  
 088 tion that dynamically learns adaptive confidence targets for individual preference pairs.  
 089
- We demonstrate how a cross-entropy objective, when coupled with meta-learned targets  
 090 guided by perplexity differentials, can effectively handle both clean and noisy preference  
 092 data by adapting the optimization landscape at a sample level.  
 093
- Through comprehensive experiments on standard alignment benchmarks, we show that  
 094 MT-DPO significantly outperforms vanilla DPO and other state-of-the-art robust align-  
 095 ment strategies across diverse data conditions, highlighting its superior adaptability and  
 096 effectiveness.  
 097

## 098 2 PRELIMINARIES

100 OThis section provides a concise overview of the foundational concepts underpinning our proposed  
 101 method, primarily focusing on Direct Preference Optimization (DPO), the formulation of a cross-  
 102 entropy objective for preference learning, and the notion of perplexity.  
 103

### 104 2.1 DIRECT PREFERENCE OPTIMIZATION (DPO)

105 Direct Preference Optimization (DPO) Rafailov et al. (2023) has emerged as an influential offline  
 106 method for aligning Large Language Models (LLMs) with human preferences, circumventing the  
 107

need for explicit reward model training. Given a dataset  $\mathcal{D} = \{(x^{(i)}, y_w^{(i)}, y_l^{(i)})\}_{i=1}^N$  of preference tuples, where  $x$  is a prompt,  $y_w$  is the preferred (winner) response, and  $y_l$  is the dispreferred (loser) response, DPO directly optimizes the LLM policy  $\pi_\theta$ . The core idea of DPO is rooted in the Bradley-Terry preference model Bradley & Terry (1952), which posits that the probability of  $y_w$  being preferred over  $y_l$  can be expressed as  $p(y_w \succ y_l | x) = \sigma(r^*(x, y_w) - r^*(x, y_l))$ , where  $r^*$  is an underlying true reward function and  $\sigma(\cdot)$  is the sigmoid function.

DPO establishes a relationship between this implicit reward and the optimal policy  $\pi^*$  (derived from standard RLHF objectives) relative to a reference policy  $\pi_{ref}$ :

$$r^*(x, y_w) - r^*(x, y_l) = \beta \log \frac{\pi^*(y_w | x) \pi_{ref}(y_l | x)}{\pi_{ref}(y_w | x) \pi^*(y_l | x)}, \quad (1)$$

where  $\beta$  is a hyperparameter controlling the deviation from  $\pi_{ref}$ . By substituting the current policy  $\pi_\theta$  for  $\pi^*$ , DPO defines its loss function as the negative log-likelihood of the observed preferences:

$$\mathcal{L}_{DPO}(\pi_\theta; \pi_{ref}) = -\mathbb{E}_{(x, y_w, y_l) \sim \mathcal{D}} [\log \sigma(\beta h_\theta(x, y_w, y_l))], \quad (2)$$

where  $h_\theta(x, y_w, y_l)$  is the log-probability ratio of the policy  $\pi_\theta$  relative to  $\pi_{ref}$  for the winner versus the loser responses:

$$h_\theta(x, y_w, y_l) = \log \frac{\pi_\theta(y_w | x) \pi_{ref}(y_l | x)}{\pi_{ref}(y_w | x) \pi_\theta(y_l | x)}. \quad (3)$$

Minimizing this loss encourages  $\pi_\theta$  to assign a higher likelihood to  $y_w$  and a lower likelihood to  $y_l$ , relative to  $\pi_{ref}$ , for each prompt  $x$ .

## 2.2 CROSS-ENTROPY OBJECTIVE FOR PREFERENCE LEARNING

The standard DPO loss (Eq. 2), maximizing the log-likelihood of observed preferences, implicitly assumes a target probability of 1 for the preferred response  $y_w$  over  $y_l$ . This inherent assumption makes it sensitive to noisy or ambiguous preference labels common in real-world data, where the observed preference may not hold with full certainty.

To overcome this limitation and enable robust learning under uncertainty, we reformulate the preference learning objective using a binary cross-entropy (BCE) loss. This formulation explicitly separates the model’s predicted preference probability,  $P_{\text{model}}(y_1 \succ y_2 | x; \theta)$ , from the desired target confidence,  $\hat{p} = p_{\text{target}}(y_1 \succ y_2 | x)$ :

$$P_{\text{model}}(y_1 \succ y_2 | x; \theta) = \sigma(\beta h_\theta(x, y_1, y_2)). \quad (4)$$

The BCE loss then minimizes the divergence between the model’s prediction and the target  $\hat{p}$ :

$$\begin{aligned} \mathcal{L}_{BCE}(\pi_\theta; \pi_{ref}, \hat{p}) = -\mathbb{E}_{(x, y_1, y_2, \hat{p}) \sim \mathcal{D}} & \left[ \hat{p} \log P_{\text{model}}(y_1 \succ y_2 | x; \theta) \right. \\ & \left. + (1 - \hat{p}) \log (1 - P_{\text{model}}(y_1 \succ y_2 | x; \theta)) \right]. \end{aligned} \quad (5)$$

Crucially, this BCE framework provides the necessary flexibility to move beyond the fixed target of 1 implicit in standard DPO. By allowing  $\hat{p}$  to vary, we can modulate the learning signal based on the perceived reliability of each preference pair, aiming to align the policy  $\pi_\theta$ ’s implied probability  $P_{\text{model}}$  with a more nuanced confidence level.

The challenge, then, lies in determining appropriate values for the target  $\hat{p}$ . One approach, exemplified by Conservative DPO (cDPO) Mitchell (2023), involves using *static*, pre-defined targets derived from global assumptions like a known noise rate (e.g., setting  $\hat{p} = 1 - \epsilon > 0.5$ , if  $y_1$  is the nominal winner and  $\epsilon$  is the assumed noise rate). While this offers some robustness, relying on global, static targets fails to capture the instance-specific variations in label quality.

In contrast, our proposed method, MT-DPO, leverages the flexibility of the BCE objective (Eq. 5) in a fundamentally different way. Instead of pre-specifying  $\hat{p}$ , MT-DPO views it as a dynamic, sample-specific confidence target  $\hat{p}_n$  spanning the full spectrum  $[0, 1]$ . Most importantly, MT-DPO *learns* this target  $\hat{p}_n$  adaptively for each instance  $n$  via a meta-learning process guided by intrinsic signals of data quality. This learned, adaptive nature of the target is central to MT-DPO’s ability to robustly handle diverse and potentially non-uniform data imperfections, forming a core contribution of our work.

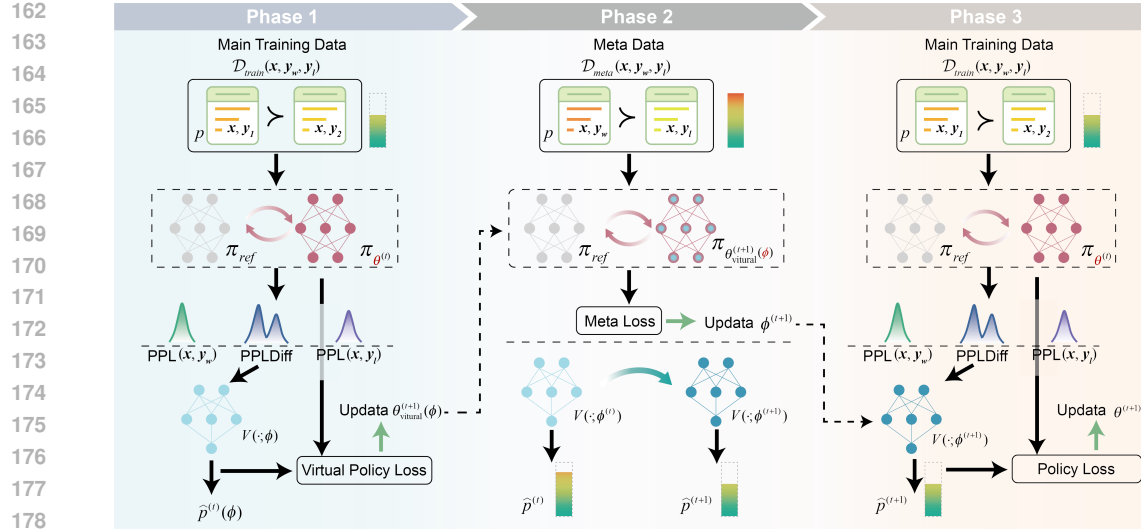


Figure 1: Overall architecture of the Meta-Target DPO (MT-DPO) framework. The confidence prediction module  $V(\cdot; \phi)$  generates a sample-specific target  $\hat{p}$  based on PPLDiff. The policy LLM  $\pi_\theta$  is updated using a cross-entropy loss with this dynamic target. The confidence module itself is updated via a meta-learning loop guided by a clean meta-dataset  $\mathcal{D}_{meta}$ .

### 3 METHODOLOGY

Building upon the preliminaries, we now introduce our proposed framework, Meta-Target DPO (MT-DPO), for robust preference alignment. MT-DPO leverages a meta-learning approach to dynamically generate adaptive confidence targets for a cross-entropy based DPO objective, guided by intrinsic signals of preference consistency.

#### 3.1 OVERALL FRAMEWORK

Aligning Large Language Models (LLMs) with human preferences under noisy or ambiguous data conditions presents a significant challenge, as static rules or global noise estimates often lack adaptability. Our proposed Meta-Target DPO (MT-DPO) framework tackles this by learning an adaptive, sample-specific confidence target,  $\hat{p}_n$ , for each preference pair. This target dynamically reflects the inferred belief in the correctness of the observed preference.

As depicted in Figure 1, MT-DPO revolves around three interacting components: a base policy LLM ( $\pi_\theta$ ) optimized via a cross-entropy loss with these dynamic targets; a confidence prediction module ( $V(\cdot; \phi)$ ) that generates  $\hat{p}_n$  from instance features; and a meta-learning procedure that refines  $\phi$  using a small, clean meta-dataset ( $\mathcal{D}_{meta}$ ). This orchestrated interplay ensures that the policy learns from adaptively calibrated preference signals, enhancing alignment robustness. Subsequent sections will detail each component of this framework.

#### 3.2 ADAPTIVE CROSS-ENTROPY OBJECTIVE FOR POLICY LEARNING

The policy LLM  $\pi_\theta$  in MT-DPO is trained to minimize a cross-entropy loss, similar in form to Eq. 5, but with the crucial difference that the target probability  $\hat{p}$  is now a sample-specific, learned value  $\hat{p}_n$  predicted by the confidence module  $V(I_n; \phi)$ , where  $I_n$  represents the input features for sample  $n$ . Let  $P_{model}(y_1^{(n)} \succ y_2^{(n)} | x^{(n)}; \theta)$  be the policy’s implied preference probability for sample  $n$ , as defined in Eq. 4. The objective for updating  $\pi_\theta$  is:

$$\mathcal{L}_{policy}(\theta, \phi) = -\mathbb{E}_{(x^{(n)}, y_1^{(n)}, y_2^{(n)}) \sim \mathcal{D}_{train}} \left[ \hat{p}_n \log P_{model}(y_1^{(n)} \succ y_2^{(n)} | x^{(n)}; \theta) + (1 - \hat{p}_n) \log(1 - P_{model}(y_1^{(n)} \succ y_2^{(n)} | x^{(n)}; \theta)) \right], \quad (6)$$

where  $\hat{p}_n = V(I_n; \phi)$ . By dynamically adjusting  $\hat{p}_n$ , this objective allows MT-DPO to adaptively modulate the learning process. If the confidence module assigns  $\hat{p}_n \approx 1$ , the loss term encourages  $\pi_\theta$  to strongly prefer  $y_1^{(n)}$  over  $y_2^{(n)}$ . Conversely, if  $\hat{p}_n \approx 0$ , it encourages the opposite preference,

effectively correcting for a perceived label error. Intermediate values of  $\hat{p}_n$  lead to a down-weighting of the sample's influence, suitable for ambiguous or highly uncertain pairs.

### 3.3 CONFIDENCE MODULE INPUT: PERPLEXITY DIFFERENTIALS

The effectiveness of the confidence module  $V(\cdot; \phi)$  hinges on informative input features  $I_n$  that correlate with preference label quality or consistency. Inspired by the findings in Kong et al. (2024), we primarily utilize the perplexity difference (PPLDiff) between the two responses in a preference pair. Given a preference pair  $(x^{(n)}, y_1^{(n)}, y_2^{(n)})$  and an anchored reference language model  $\pi_{\text{anchor}}$  (which could be the initial SFT model  $\pi_{\text{ref}}$ , or a separate model periodically updated on clean data, as in Kong et al. (2024)), the PPLDiff is computed as:

$$\text{PPLDiff}^{(n)} = \log \text{PPL}(x^{(n)}, y_1^{(n)}; \pi_{\text{anchor}}) - \log \text{PPL}(x^{(n)}, y_2^{(n)}; \pi_{\text{anchor}}). \quad (7)$$

Here,  $\text{PPL}(x, y; \pi_{\text{anchor}})$  denotes the perplexity of the concatenated sequence  $[x; y]$  under the model  $\pi_{\text{anchor}}$ , calculated as the exponential of the average negative log-likelihood of the sequence. Intuitively, if  $y_1^{(n)}$  is genuinely preferred and consistent with aligned language, its PPL should be lower than that of  $y_2^{(n)}$ , leading to a negative PPLDiff. Conversely, if  $y_1^{(n)}$  is noisy (i.e.,  $y_2^{(n)}$  is actually better), its PPL might be higher, resulting in a positive PPLDiff. A PPLDiff close to zero might indicate ambiguity or similar quality. This PPLDiff value serves as a primary input  $I_n$  to our confidence module  $V(\cdot; \phi)$ , which is typically a small multi-layer perceptron (MLP) outputting a value in  $[0, 1]$ . Other auxiliary features, such as response lengths or initial policy log-probabilities, could also be incorporated into  $I_n$ . The choice of  $\pi_{\text{anchor}}$  is crucial; in our main experiments, we use the SFT model, and we provide a detailed analysis of this choice in Appendix E.1.

### 3.4 META-LEARNING PROCEDURE FOR CONFIDENCE MODULE

The parameters  $\phi$  of the confidence module  $V(\cdot; \phi)$  are learned through a meta-optimization process, akin to the strategy in Meta-Weight-Net Shu et al. (2019). This process requires a small, trusted meta-dataset  $\mathcal{D}_{\text{meta}} = \{(x^{(m)}, y_w^{(m)}, y_l^{(m)})\}_{m=1}^M$  consisting of clean preference pairs, where  $y_w^{(m)}$  is definitively preferred over  $y_l^{(m)}$ .

The meta-learning proceeds iteratively within each training iteration  $t$ . The process involves three key steps:

First, for a mini-batch  $\mathcal{B}_{\text{train}}$  from  $\mathcal{D}_{\text{train}}$ , confidence targets  $\hat{p}_n^{(t)} = V(I_n; \phi^{(t)})$  are computed using the current confidence module parameters  $\phi^{(t)}$ . A hypothetical (virtual) update of the policy parameters  $\theta^{(t)}$  is then performed by taking one gradient step on the policy loss  $\mathcal{L}_{\text{policy}}(\theta^{(t)}, \phi^{(t)})$  with respect to  $\theta^{(t)}$  on  $\mathcal{B}_{\text{train}}$ . This results in the virtual policy parameters:

$$\theta_{\text{virtual}}^{(t+1)}(\phi^{(t)}) = \theta^{(t)} - \alpha \nabla_{\theta^{(t)}} \mathcal{L}_{\text{policy}}(\theta^{(t)}, \phi^{(t)}). \quad (8)$$

It is crucial to note that  $\theta_{\text{virtual}}^{(t+1)}$  remains a function of  $\phi^{(t)}$  because the policy loss  $\mathcal{L}_{\text{policy}}$  depends on the targets  $\hat{p}_n^{(t)}$ , which are generated by  $V(I_n; \phi^{(t)})$ .

Next, the performance of this virtual policy  $\theta_{\text{virtual}}^{(t+1)}(\phi^{(t)})$  is evaluated on a mini-batch  $\mathcal{B}_{\text{meta}}$  sampled from the clean meta-dataset  $\mathcal{D}_{\text{meta}}$ . The meta-objective is the standard DPO loss, as preferences in  $\mathcal{D}_{\text{meta}}$  are assumed to be clean (effectively implying  $\hat{p} = 1$  for these pairs). This meta-loss, which depends on  $\phi^{(t)}$  through  $\theta_{\text{virtual}}^{(t+1)}$ , is defined as:

$$\mathcal{L}_{\text{meta}}(\phi^{(t)}) = \mathcal{L}_{\text{DPO}}(\pi_{\theta_{\text{virtual}}^{(t+1)}(\phi^{(t)})}; \pi_{\text{ref}}). \quad (9)$$

The parameters  $\phi$  of the confidence module are then updated by descending the gradient of this meta-loss with respect to  $\phi^{(t)}$ :

$$\phi^{(t+1)} = \phi^{(t)} - \eta \nabla_{\phi^{(t)}} \mathcal{L}_{\text{meta}}(\phi^{(t)}), \quad (10)$$

where  $\eta$  is the meta-learning rate. The gradient  $\nabla_{\phi^{(t)}} \mathcal{L}_{\text{meta}}(\phi^{(t)})$  is computed via backpropagation through the virtual policy update step (Eq. 8).

Finally, the actual policy parameters  $\theta$  are updated. This update uses the newly refined confidence module parameters  $\phi^{(t+1)}$  to compute fresh confidence targets  $\hat{p}_n^{(t+1)} = V(I_n; \phi^{(t+1)})$  for the original training mini-batch  $\mathcal{B}_{train}$ . The policy parameters are then updated by descending the gradient of  $\mathcal{L}_{policy}(\theta^{(t)}, \phi^{(t+1)})$  with respect to  $\theta^{(t)}$ :

$$\theta^{(t+1)} = \theta^{(t)} - \alpha \nabla_{\theta^{(t)}} \mathcal{L}_{policy}(\theta^{(t)}, \phi^{(t+1)}). \quad (11)$$

This iterative process enables  $V(\cdot; \phi)$  to learn to assign confidence targets  $\hat{p}_n$  that, when utilized in  $\mathcal{L}_{policy}$ , guide the policy  $\pi_\theta$  towards improved performance on trusted, clean preference data. The overall training algorithm is summarized in Appendix A. Further theoretical analysis, including a generalization bound for the meta-learned confidence module, is provided in Appendix B.

## 4 EXPERIMENTS

We conduct experiments to evaluate our proposed Meta-Target DPO (MT-DPO) framework, focusing on its effectiveness and robustness in aligning LLMs with human preferences compared to relevant baselines.

### 4.1 EXPERIMENTAL SETUP

**Datasets and Noise Simulation.** Our evaluations are performed on two standard preference datasets: Golden HH dataset Bai et al. (2022a;b) and OASST1 Stiennon et al. (2020); Völske et al. (2017), using their standard splits. To assess robustness, we introduce symmetric label noise to the training sets by randomly flipping preference labels with probabilities  $\epsilon_{noise} \in \{0\% \text{ (clean)}, 10\%, 20\%, 30\%, 40\%\}$ , following protocols from Mitchell (2023); Kong et al. (2024); Liang et al. (2024). For MT-DPO’s meta-learning, a small, clean meta-dataset  $\mathcal{D}_{meta}$  is sampled and held out, as suggested by Kong et al. (2024); Shu et al. (2019).

**Baselines and Evaluation.** We compare MT-DPO against several strong baselines: Vanilla DPO Rafailov et al. (2023), GDPO (with fixed  $\hat{p} = 0.75$ ) Furuta et al. (2024), Conservative DPO (cDPO, with oracle  $\epsilon_{noise}$  for noisy settings and  $\hat{p} = 1.0$  for clean) Mitchell (2023), Robust DPO (rDPO) Liang et al. (2024), and PerpCorrect-DPO Kong et al. (2024) (DPO on data denoised by PerpCorrect using  $\mathcal{D}_{meta}$ ). All DPO-based methods share the same base LLM architecture and an SFT-derived reference policy  $\pi_{ref}$  for fair comparison. Performance is primarily measured by win rate (%) against the SFT model on test sets, evaluated by an independent LLM judge (GPT-4) following Rafailov et al. (2023); Lee et al. (2023). Further details on dataset processing, specific baseline configurations (including GDPO variants), and precise evaluation protocols are provided in Appendix C.

### 4.2 IMPLEMENTATION DETAILS

**Base Models and SFT:** We use pre-trained LLMs such as Llama-2-7B Touvron et al. (2023) or phi-2 Javaheripi et al. (2023) as our base models. Prior to DPO-style alignment, these models are first supervised fine-tuned (SFT) on the preferred responses ( $y_w$ ) from the clean training portion of the respective datasets. This SFT model then serves as the initial policy  $\theta^{(0)}$  and the reference policy  $\pi_{ref}$  for all DPO methods, including MT-DPO. The SFT model also acts as the default anchored model  $\pi_{anchor}$  for PPLDiff computation in MT-DPO and PerpCorrect-DPO, unless otherwise specified.

**MT-DPO Configuration and Training:** Our MT-DPO’s confidence prediction module  $V(\cdot; \phi)$  is implemented as a small MLP (typically with one or two hidden layers and a final sigmoid activation) with the perplexity difference (PPLDiff), potentially normalized, as its primary input  $I_n$ . The SFT model serves as the default anchored model  $\pi_{anchor}$  for PPLDiff computation. We use the AdamW optimizer for both the policy LLM  $\theta$  (learning rates typically  $1e^{-6}$  to  $5e^{-5}$ ) and the confidence module  $\phi$  (learning rates typically  $1e^{-4}$  to  $1e^{-3}$ ). The DPO hyperparameter  $\beta$  is consistently set to 0.1 across all DPO variants.

All models, including baselines, are trained for a fixed number of epochs or steps on the respective training datasets. We utilize standard deep learning libraries such as PyTorch, along with libraries from Hugging Face Transformers and TRL von Werra et al. (2020), for implementation. All experiments are conducted on NVIDIA A100 GPUs. Comprehensive hyperparameter settings for all methods and datasets, including specific learning rates and  $\mathcal{D}_{meta}$  size, are detailed in Appendix D.

324  
325

Table 1: Win Rates (%) of Llama-2-7B Against SFT on Golden HH and OASST1 Datasets.

326  
327  
328  
329  
330  
331  
332

Method	Golden HH					OASST1				
	Clean (0%)	10%	20%	30%	40%	Clean (0%)	10%	20%	30%	40%
Vanilla DPO	97.22	92.53	82.62	68.50	53.15	97.17	96.64	92.71	90.21	86.29
GDPO ( $\hat{p} = 0.75$ )	97.57	97.15	95.53	94.26	91.21	97.52	97.06	94.21	93.08	92.73
cDPO (Oracle $\epsilon/\hat{p} = 1$ )	97.38	96.04	90.85	83.23	65.60	97.67	96.18	93.63	90.62	88.02
rDPO	97.21	96.65	95.22	93.90	90.45	97.76	95.92	93.73	92.05	90.62
PerpCorrect-DPO	97.87	97.51	96.24	95.53	94.92	98.05	96.38	94.04	93.99	93.17
<b>MT-DPO (Ours)</b>	<b>98.02</b>	<b>97.85</b>	<b>97.31</b>	<b>96.58</b>	<b>95.50</b>	<b>98.55</b>	<b>97.17</b>	<b>95.54</b>	<b>94.92</b>	<b>94.28</b>

333  
334335  
336

Table 2: Win Rates (%) of Phi-2 Against SFT on Golden HH and OASST1 Datasets.

337  
338  
339  
340  
341  
342  
343

Method	Golden HH					OASST1				
	Clean (0%)	10%	20%	30%	40%	Clean (0%)	10%	20%	30%	40%
Vanilla DPO	96.50	93.19	85.57	73.07	54.98	69.12	66.94	62.61	58.44	52.42
GDPO ( $\hat{p} = 0.75$ )	97.07	97.54	96.08	94.52	85.39	68.73	67.93	63.58	59.88	53.05
cDPO (Oracle $\epsilon/\hat{p} = 1$ )	97.56	97.21	92.63	81.05	66.72	69.30	67.30	61.44	54.87	49.21
rDPO	97.01	96.49	95.73	93.34	84.55	67.16	63.95	59.47	56.45	45.20
PerpCorrect-DPO	98.18	98.17	97.05	97.66	96.39	72.55	71.34	69.04	68.27	68.49
<b>MT-DPO (Ours)</b>	<b>98.63</b>	<b>98.33</b>	<b>97.58</b>	<b>98.49</b>	<b>97.91</b>	<b>74.69</b>	<b>72.54</b>	<b>71.15</b>	<b>70.57</b>	<b>69.91</b>

344  
345  
346

## 4.2.1 MAIN PERFORMANCE COMPARISON

347  
348  
349  
350  
351  
352  
353  
354  
355  
356  
357  
358  
359

We now present the empirical results of MT-DPO and compare its performance against the baselines on both clean and noisy preference datasets. For the noisy data conditions ( $\epsilon_{\text{noise}} \in \{10\%, 20\%, 30\%, 40\%\}$ ), results for baseline methods (Vanilla DPO, cDPO, rDPO, PerpCorrect-DPO) are primarily adapted from Kong et al. (2024) Kong et al. (2024) where applicable for the respective models and datasets, unless specified otherwise by our own baseline runs. All results for our proposed MT-DPO and GDPO ( $\hat{p} = 0.75$ ), as well as all results on clean (0% noise) data across all methods, are from our own reproducible experiments. The primary metric is the win rate (%) against the SFT model, evaluated by GPT-4. All results are consolidated in Table 1 for Llama-2-7B and Table 2 for Phi-2. The improvements of our implemented models (MT-DPO and GDPO) over our SFT baseline were confirmed to be statistically significant (Wilcoxon signed-rank test,  $p < 0.01$ ). Comparisons with other baseline methods rely on their reported aggregate performance metrics and observed differences in win rates.

360  
361  
362  
363  
364

As shown in Tables 1 and 2, our proposed MT-DPO consistently achieves state-of-the-art (SOTA) performance across all evaluated conditions. On clean datasets (0% noise), MT-DPO demonstrates top-tier results, indicating its adaptive mechanism effectively handles ideal conditions without performance degradation; for example, it achieved the highest clean data win rate of 98.63% with the Phi-2 model on the Golden HH dataset.

365  
366  
367  
368  
369  
370  
371  
372

The **robustness of MT-DPO under noisy conditions** is particularly compelling. While Vanilla DPO’s performance significantly deteriorates with increasing noise, MT-DPO maintains substantially higher win rates. It consistently outperforms other robust baselines, including cDPO (Oracle), rDPO, and PerpCorrect-DPO, across most noise levels, models, and datasets. This underscores the advantage of MT-DPO’s dynamic, meta-learned target adaptation strategy in navigating imperfect preference data. For example, under 40% noise with Llama-2-7B on Golden HH, MT-DPO (95.50%) significantly surpasses Vanilla DPO (53.15%) and also leads other robust methods like PerpCorrect-DPO (94.92%).

373  
374  
375

Notably, GDPO ( $\hat{p} = 0.75$ ) also exhibits strong robustness, often outperforming cDPO and rDPO on the Golden HH dataset, suggesting the efficacy of a well-chosen conservative target. However, MT-DPO generally provides further improvements by adapting these targets at a sample level.

376  
377

In summary, the empirical results strongly validate MT-DPO as a highly effective and robust method for aligning LLMs, demonstrating superior performance and resilience to noise compared to existing approaches.

378 4.2.2 ABLATION STUDIES  
379380 To understand the contribution of different components of MT-DPO, we conducted ablation studies  
381 focusing on the impact of the meta-dataset size and the input features for the confidence module.  
382 These experiments were performed on the Golden HH dataset with 30% noise using the Llama-2-7B  
383 model.384 **Impact of Meta-Dataset Size.** We investigated MT-DPO’s sensitivity to the size of the clean meta-  
385 dataset,  $|\mathcal{D}_{meta}|$ . Table 3 presents the win rates as  $|\mathcal{D}_{meta}|$  varies.  
386387 Table 3: Impact of meta-dataset size ( $|\mathcal{D}_{meta}|$ ) on MT-DPO performance (Win rate % vs SFT) on  
388 Golden HH with  $\epsilon_{noise} = 30\%$  using Llama-2-7B.  
389

$ \mathcal{D}_{meta} $	25	50	100	150	200
MT-DPO Win Rate (%)	94.66	95.37	96.29	<b>96.58</b>	96.70

390 The results indicate that MT-DPO achieves strong performance even with a very small meta-dataset;  
391 utilizing only 50 samples for  $\mathcal{D}_{meta}$  yielded a win rate of 95.37%. This confirms the data efficiency  
392 of the meta-learning guidance, consistent with findings in Shu et al. (2019); Kong et al. (2024).  
393 While performance improves with more meta-data, the gains diminish beyond approximately 150  
394 samples (96.58%), suggesting that a modest amount of clean data is sufficient for the confidence  
395 module to learn effective target calibration strategies. Increasing  $|\mathcal{D}_{meta}|$  to 200 resulted in only a  
396 marginal improvement to 96.70%.  
397400 **Importance of PPLDiff as Input Feature.** To verify the utility of PPLDiff as the primary input  
401 feature  $I_n$  for the confidence module, we compared the full MT-DPO against two variants: (1) MT-  
402 DPO-NoFeat, where the confidence module learns a global  $\hat{p}$  without sample-specific input features,  
403 and (2) MT-DPO-Loss, which uses the sample’s DPO loss from a prior iteration as input, similar to  
404 Shu et al. (2019). Table 4 shows these results.  
405406 Table 4: Impact of input features for the confidence module on MT-DPO performance (Win rate %  
407 vs SFT) on Golden HH with  $\epsilon_{noise} = 30\%$  using Llama-2-7B.  
408

Feature for Confidence Module $V(\cdot; \phi)$	Win Rate (%)
No Features (Global $\hat{p}$ learned)	93.58
DPO Loss Value (MT-DPO-Loss)	94.83
PPLDiff (Full MT-DPO)	<b>96.58</b>

413 The results in Table 4 clearly demonstrate that utilizing PPLDiff as an input feature significantly  
414 enhances MT-DPO’s performance. The full MT-DPO (96.58%) substantially outperforms both the  
415 MT-DPO-Loss variant (94.83%) and the MT-DPO-NoFeat variant (93.58%). This underscores the  
416 effectiveness of PPLDiff as a reliable indicator of preference consistency and label quality, enabling  
417 the confidence module to learn more accurate and beneficial sample-specific targets  $\hat{p}_n$ .  
418419 4.2.3 ANALYSIS OF LEARNED CONFIDENCE TARGETS  
420421 To gain deeper insight into the adaptive mechanism of MT-DPO, we analyzed the behavior of the  
422 learned confidence targets  $\hat{p}_n$  generated by the trained confidence module  $V(\cdot; \phi)$ . This investigation  
423 focuses on understanding how the module assigns these targets in response to varying perceived label  
424 quality and how these assignments correlate with PPLDiff. For this analysis, we utilized a subset  
425 of the Golden HH training data where 30% symmetric label noise was introduced. After training  
426 MT-DPO (Llama-2-7B), we passed samples from this noisy training subset through the converged  
427 confidence module.428 Figure 2 presents a combined visualization. Figure 2a illustrates the distributions of learned  $\hat{p}_n$  for  
429 samples known to be “Clean” (original label preserved) versus “Noisy (Flipped)” (label intention-  
430 ally flipped). A clear separation is anticipated: clean samples should have  $\hat{p}_n$  concentrated near  
431 1.0, while noisy samples should have  $\hat{p}_n$  skewed towards 0.0. Figure 2b presents a scatter plot of  
432  $\hat{p}_n$  against PPLDiff. A negative correlation is expected: instances with strongly negative PPLDiff

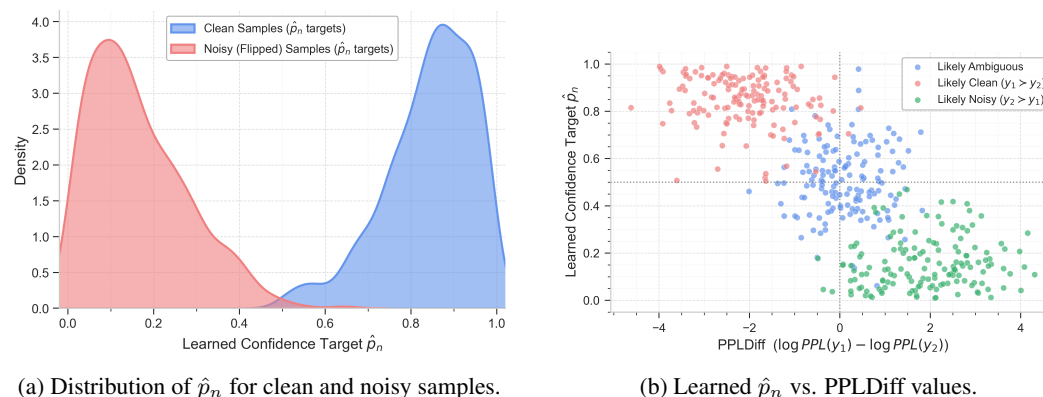


Figure 2: Analysis of learned confidence targets  $\hat{p}_n$  from MT-DPO on Golden HH with 30% noise (Llama-2-7B). (a) Distinct distributions of  $\hat{p}_n$  for known clean and noisy samples. (b) Negative correlation between PPLDiff and learned  $\hat{p}_n$ .

(suggesting  $y_1$  is more likely under  $\pi_{\text{anchor}}$ ) should receive  $\hat{p}_n \approx 1.0$ , while positive PPLDiff values should correlate with  $\hat{p}_n \approx 0.0$ .

This qualitative analysis is intended to support the hypothesis that the meta-learned confidence module in MT-DPO learns an interpretable and effective mapping from PPLDiff to adaptive confidence targets. This ability to differentiate preference signals and modulate the learning objective accordingly is key to MT-DPO’s robust performance. Further details on this analysis and illustrative case studies demonstrating the mechanism in action are provided in Appendix E.2 and F.

### 4.3 CONCLUSION

We introduced Meta-Target DPO (MT-DPO), a novel meta-learning framework for robust preference alignment. MT-DPO dynamically learns adaptive, sample-specific confidence targets for a cross-entropy DPO objective, guided by signals like perplexity differentials and a small clean meta-dataset. This allows intelligent modulation of the learning signal per preference pair, effectively handling diverse label quality. Experiments showed MT-DPO significantly outperforms standard DPO and robust baselines on clean and noisy datasets, highlighting its adaptability in achieving reliable LLM alignment under uncertainty. While MT-DPO demonstrates strong results, its efficacy relies on the quality of the small meta-dataset, and the meta-learning process introduces some computational overhead compared to simpler DPO variants. Future work includes exploring richer input features for the confidence module, investigating sensitivity to meta-dataset characteristics, and extending MT-DPO to other preference learning paradigms. MT-DPO offers a principled direction for building more resilient AI systems from imperfect human feedback.

486 ETHICS STATEMENT  
487488 In accordance with ICLR policy, we disclose that large language models (LLMs) were employed  
489 as writing assistants during the preparation of this paper. Their primary function was to support  
490 grammar correction and language refinement, with the goal of improving the overall readability of  
491 the manuscript. All core ideas and analyses were conceived and developed solely by the human  
492 authors, who assume full responsibility for the final content of the paper.  
493494 REFERENCES  
495496 Amanda Askell, Yuntao Bai, Anna Chen, Dawn Drain, Deep Ganguli, Tom Henighan, Andy Jones,  
497 Nicholas Joseph, Ben Mann, Nova DasSarma, et al. A general language assistant as a laboratory  
498 for alignment. *arXiv preprint arXiv:2112.00861*, 2021.500 Mohammad Gheshlaghi Azar, Mark Rowland, Bilal Piot, Daniel Guo, Daniele Calandriello, Michal  
501 Valko, and Rémi Munos. A general theoretical paradigm to understand learning from human  
502 preferences. *arXiv preprint arxiv:2310.12036*, 2023.503 Yuntao Bai, Andy Jones, Kamal Ndousse, Amanda Askell, Anna Chen, Nova DasSarma, Dawn  
504 Drain, Stanislav Fort, Deep Ganguli, Tom Henighan, Nicholas Joseph, Saurav Kadavath, Jackson  
505 Kernion, Tom Conerly, Sheer El-Showk, Nelson Elhage, Zac Hatfield-Dodds, Danny Hernandez,  
506 Tristan Hume, Scott Johnston, Shauna Kravec, Liane Lovitt, Neel Nanda, Catherine Olsson,  
507 Dario Amodei, Tom Brown, Jack Clark, Sam McCandlish, Chris Olah, Ben Mann, and Jared Kaplan.  
508 Training a helpful and harmless assistant with reinforcement learning from human feedback.  
509 *arXiv preprint arXiv:2204.05862*, 2022a.510 Yuntao Bai, Saurav Kadavath, Sandipan Kundu, Amanda Askell, Jackson Kernion, Andy Jones,  
511 Anna Chen, Anna Goldie, Azalia Mirhoseini, Cameron McKinnon, Carol Chen, Catherine Olson,  
512 Christopher Olah, Danny Hernandez, Dawn Drain, Deep Ganguli, Dustin Li, Eli Tran-  
513 Johnson, Ethan Perez, Jamie Kerr, Jared Mueller, Jeffrey Ladish, Joshua Landau, Kamal Ndousse,  
514 Kamile Lukosuite, Liane Lovitt, Michael Sellitto, Nelson Elhage, Nicholas Schiefer, Noemi Mercado,  
515 Nova DasSarma, Robert Lasenby, Robin Larson, Sam Ringer, Scott Johnston, Shauna Kravec,  
516 Sheer El Showk, Stanislav Fort, Tamera Lanham, Timothy Telleen-Lawton, Tom Conerly,  
517 Tom Henighan, Tristan Hume, Samuel R. Bowman, Zac Hatfield-Dodds, Ben Mann, Dario  
518 Amodei, Nicholas Joseph, Sam McCandlish, Tom Brown, and Jared Kaplan. Constitutional ai:  
519 Harmlessness from ai feedback. *arXiv preprint arXiv:2212.08073*, 2022b.520 Ralph Allan Bradley and Milton E. Terry. Rank analysis of incomplete block designs: I. the method  
521 of paired comparisons. *Biometrika*, 39(3/4):324–345, 1952.523 Stephen Casper, Xander Davies, Claudia Shi, Thomas Krendl Gilbert, Jérémie Scheurer, Javier  
524 Rando, Rachel Freedman, Tomek Korbak, David Lindner, Pedro Freire, Tony Tong Wang, Samuel  
525 Marks, Charbel-Raphael Segerie, Micah Carroll, Andi Peng, Phillip J.K. Christoffersen, Mehul  
526 Damani, Stewart Slocum, Usman Anwar, Anand Siththanjan, Max Nadeau, Eric J Michaud,  
527 Jacob Pfau, Dmitrii Krasheninnikov, Xin Chen, Lauro Langosco, Peter Hase, Erdem Biyik, Anca  
528 Dragan, David Krueger, Dorsa Sadigh, and Dylan Hadfield-Menell. Open problems and funda-  
529 mental limitations of reinforcement learning from human feedback. *Transactions on Machine  
530 Learning Research*, pp. 2835–8856, 2023.531 Angelica Chen, Sadhika Malladi, Lily Zhang, Xinyi Chen, Qiuyi Richard Zhang, Rajesh Ran-  
532 ganath, and Kyunghyun Cho. Preference learning algorithms do not learn preference rankings. In  
533 *NeurIPS*, volume 37, pp. 101928–101968, 2024.535 Paul Christiano, Jan Leike, Tom B. Brown, Miljan Martic, Shane Legg, and Dario Amodei. Deep  
536 reinforcement learning from human preferences. *arXiv preprint arXiv:1706.03741*, 2017.538 Hyung Won Chung, Le Hou, Shayne Longpre, Barret Zoph, Yi Tay, William Fedus, Yunxuan Li,  
539 Xuezhi Wang, Mostafa Dehghani, Siddhartha Brahma, et al. Scaling instruction-finetuned lan-  
guage models. *Journal of Machine Learning Research*, 25(70):1–53, 2024.

540 Jacob Eisenstein, Jonathan Berant, Chirag Nagpal, Alekh Agarwal, Ahmad Beirami, Alexander  
 541 Nicholas D'Amour, Krishnamurthy Dj Dvijotham, Katherine A Heller, Stephen Robert Pfohl,  
 542 and Deepak Ramachandran. Reward model underspecification in language model alignment. In  
 543 *NeurIPS Workshop*, 2023.

544 Kawin Ethayarajh, Winnie Xu, Niklas Muennighoff, Dan Jurafsky, and Douwe Kiela. Kto: Model  
 545 alignment as prospect theoretic optimization. *arXiv preprint arXiv:2402.01306*, 2024.

546 Hiroki Furuta, Kuang-Huei Lee, Shixiang Shane Gu, Yutaka Matsuo, Aleksandra Faust, Heiga Zen,  
 547 and Izzeddin Gur. Geometric-averaged preference optimization for soft preference labels. In  
 548 *NeurIPS*, volume 37, pp. 57076–57114, 2024.

549 Yang Gao, Dana Alon, and Donald Metzler. Impact of preference noise on the alignment performance  
 550 of generative language models. *arXiv preprint arXiv:2404.09824*, 2024.

551 Bo Han, Quanming Yao, Tongliang Liu, Gang Niu, Ivor W Tsang, James T Kwok, and Masashi  
 552 Sugiyama. A survey of label-noise representation learning: Past, present and future. *arXiv  
 553 preprint arXiv:2011.04406*, 2020.

554 David R Hunter. Mm algorithms for generalized bradley-terry models. *The annals of statistics*, 32  
 555 (1):384–406, 2004.

556 Mojan Javaheripi, Sébastien Bubeck, Marah Abdin, Jyoti Aneja, Sébastien Bubeck, Caio  
 557 César Teodoro Mendes, Weizhu Chen, Allie Del Giorno, Ronen Eldan, Sivakanth Gopi, et al.  
 558 Phi-2: The surprising power of small language models. *Microsoft Research Blog*, 1(3):3, 2023.

559 Lu Jiang, Zhengyuan Zhou, Thomas Leung, Li-Jia Li, and Li Fei-Fei. Mentornet: Learning data-  
 560 driven curriculum for very deep neural networks on corrupted labels. In *ICML*, pp. 2304–2313,  
 561 2018.

562 Keyi Kong, Xilie Xu, Di Wang, Jingfeng Zhang, and Mohan S Kankanhalli. Perplexity-aware  
 563 correction for robust alignment with noisy preferences. In *NeurIPS*, volume 37, pp. 28296–28321,  
 564 2024.

565 Andreas Köpf, Yannic Kilcher, Dimitri von Rütte, Sotiris Anagnostidis, Zhi Rui Tam, Keith Stevens,  
 566 Abdullah Barhoum, Duc Nguyen, Oliver Stanley, Richárd Nagyfi, Shahul ES, Sameer Suri, David  
 567 Glushkov, Arnav Dantuluri, Andrew Maguire, Christoph Schuhmann, Huu Nguyen, and Alexander  
 568 Mattick. Openassistant conversations - democratizing large language model alignment. In  
 569 *NeurIPS*, volume 36, pp. 47669–47681, 2023.

570 Harrison Lee, Samrat Phatale, Hassan Mansoor, Thomas Mesnard, Johan Ferret, Kellie Lu, Colton  
 571 Bishop, Ethan Hall, Victor Carbune, Abhinav Rastogi, and Sushant Prakash. Rlaif: Scaling re-  
 572 enforcement learning from human feedback with ai feedback. *arXiv preprint arXiv:2309.00267*,  
 573 2023.

574 Xize Liang, Chao Chen, Jie Wang, Yue Wu, Zhihang Fu, Zhihao Shi, Feng Wu, and Jieping  
 575 Ye. Robust preference optimization with provable noise tolerance for llms. *arXiv preprint  
 576 arXiv:2404.04102*, 2024.

577 Eric Mitchell. A note on dpo with noisy preferences & relationship to ipo, 2023. URL <https://ericmitchell.ai/cdpo.pdf>.

578 Long Ouyang, Jeff Wu, Xu Jiang, Diogo Almeida, Carroll L. Wainwright, Pamela Mishkin, Chong  
 579 Zhang, Sandhini Agarwal, Katarina Slama, Alex Ray, John Schulman, Jacob Hilton, Fraser Kel-  
 580 ton, Luke Miller, Maddie Simens, Amanda Askell, Peter Welinder, Paul Christiano, Jan Leike,  
 581 and Ryan Lowe. Training language models to follow instructions with human feedback. *arXiv  
 582 preprint arXiv:2203.02155*, 2022.

583 Rafael Rafailov, Archit Sharma, Eric Mitchell, Christopher D Manning, Stefano Ermon, and Chelsea  
 584 Finn. Direct preference optimization: Your language model is secretly a reward model. In *Thirty-  
 585 seventh Conference on Neural Information Processing Systems*, 2023.

586 Jun Shu, Qi Xie, Lixuan Yi, Qian Zhao, Sanping Zhou, Zongben Xu, and Deyu Meng. Meta-weight-  
 587 net: Learning an explicit mapping for sample weighting. In *NeurIPS*, volume 32, 2019.

594 Hwanjun Song, Minseok Kim, Dongmin Park, Yooju Shin, and Jae-Gil Lee. Learning from noisy  
 595 labels with deep neural networks: A survey. *IEEE Transactions on Neural Networks and Learning*  
 596 *Systems*, 34(11):8135–8153, 2022.

597

598 Nisan Stiennon, Long Ouyang, Jeff Wu, Daniel M. Ziegler, Ryan Lowe, Chelsea Voss, Alec Radford,  
 599 Dario Amodei, and Paul Christiano. Learning to summarize from human feedback. *arXiv preprint*  
 600 *arXiv:2009.01325*, 2020.

601 Hugo Touvron, Louis Martin, Kevin Stone, Peter Albert, Amjad Almahairi, Yasmine Babaei, Niko-  
 602 lay Bashlykov, Soumya Batra, Prajjwal Bhargava, Shruti Bhosale, Dan Bikel, Lukas Blecher,  
 603 Cristian Canton Ferrer, Moya Chen, Guillem Cucurull, David Esiobu, Jude Fernandes, Jeremy  
 604 Fu, Wenjin Fu, Brian Fuller, Cynthia Gao, Vedanuj Goswami, Naman Goyal, Anthony Hartshorn,  
 605 Saghar Hosseini, Rui Hou, Hakan Inan, Marcin Kardas, Viktor Kerkez, Madian Khabsa, Isabel  
 606 Kloumann, Artem Korenev, Punit Singh Koura, Marie-Anne Lachaux, Thibaut Lavril, Jenya Lee,  
 607 Diana Liskovich, Yinghai Lu, Yuning Mao, Xavier Martinet, Todor Mihaylov, Pushkar Mishra,  
 608 Igor Molybog, Yixin Nie, Andrew Poulton, Jeremy Reizenstein, Rashi Rungta, Kalyan Saladi,  
 609 Alan Schelten, Ruan Silva, Eric Michael Smith, Ranjan Subramanian, Xiaoqing Ellen Tan, Binh  
 610 Tang, Ross Taylor, Adina Williams, Jian Xiang Kuan, Puxin Xu, Zheng Yan, Iliyan Zarov, Yuchen  
 611 Zhang, Angela Fan, Melanie Kambadur, Sharan Narang, Aurelien Rodriguez, Robert Stojnic,  
 612 Sergey Edunov, and Thomas Scialom. Llama 2: Open foundation and fine-tuned chat models,  
 613 2023. URL <https://arxiv.org/abs/2307.09288>.

614 Anna Vettoruzzo, Mohamed-Rafik Bouguelia, Joaquin Vanschoren, Thorsteinn Rögnvaldsson, and  
 615 KC Santosh. Advances and challenges in meta-learning: A technical review. *IEEE Transactions*  
 616 *on Pattern Analysis and Machine Intelligence*, 46(7):4763–4779, 2024.

617 Michael Völske, Martin Potthast, Shahbaz Syed, and Benno Stein. TL;DR: Mining Reddit to learn  
 618 automatic summarization. In *Proceedings of the Workshop on New Frontiers in Summarization*,  
 619 pp. 59–63, 2017.

620 Leandro von Werra, Younes Belkada, Lewis Tunstall, Edward Beeching, Tristan Thrush, Nathan  
 621 Lambert, Shengyi Huang, Kashif Rasul, and Quentin Gallouédec. Trl: Transformer reinforcement  
 622 learning. <https://github.com/huggingface/trl>, 2020.

623

624 Chuhuan Wu, Fangzhao Wu, Tao Qi, Yongfeng Huang, and Xing Xie. Noisytune: A little noise can  
 625 help you finetune pretrained language models better. In *ACL*, pp. 680–685, 2022.

626 Junkang Wu, Yuexiang Xie, Zhengyi Yang, Jiancan Wu, Jinyang Gao, Bolin Ding, Xiang Wang,  
 627 and Xiangnan He. \beta-dpo: Direct preference optimization with dynamic \beta. In *NeurIPS*,  
 628 volume 37, pp. 129944–129966, 2024.

629

630 Sen Zhao, Mahdi Milani Fard, Harikrishna Narasimhan, and Maya Gupta. Metric-optimized exam-  
 631 ple weights. In *International Conference on Machine Learning*, pp. 7533–7542. PMLR, 2019.

632 Daniel M Ziegler, Nisan Stiennon, Jeffrey Wu, Tom B Brown, Alec Radford, Dario Amodei, Paul  
 633 Christiano, and Geoffrey Irving. Fine-tuning language models from human preferences. *arXiv*  
 634 *preprint arXiv:1909.08593*, 2019.

635

636

637

638

639

640

641

642

643

644

645

646

647

648 **A ALGORITHM DETAILS**  
649650 **Algorithm 1** MT-DPO Training Procedure  
651

---

652 1: **Input:** Initial policy  $\theta^{(0)}$ , initial confidence module  $\phi^{(0)}$ , reference  $\pi_{ref}$ , (optional) anchor  
653  $\pi_{anchor}$ , training data  $\mathcal{D}_{train}$ , meta-data  $\mathcal{D}_{meta}$ , learning rates  $\alpha, \eta$ , iterations  $T$ .  
654 2: **Output:** Trained policy parameters  $\theta^{(T)}$ .  
655 3: **for**  $t = 0, 1, \dots, T - 1$  **do**  
656 4:     Sample mini-batch  $\mathcal{B}_{train}$  from  $\mathcal{D}_{train}$ ; Sample mini-batch  $\mathcal{B}_{meta}$  from  $\mathcal{D}_{meta}$ .  
657 5:     For  $n \in \mathcal{B}_{train}$ , compute features  $I_n$  (e.g., PPLDiff using  $\pi_{anchor}$ ).  
658 6:     // — Virtual Policy Update —  
659 7:     Compute confidence targets  $\hat{p}_n^{(t)} = V(I_n; \phi^{(t)})$  for samples in  $\mathcal{B}_{train}$ .  
660 8:     Compute virtual policy parameters  $\theta_{\text{virtual}}^{(t+1)}(\phi^{(t)})$  using  $\mathcal{B}_{train}$  with targets  $\hat{p}_n^{(t)}$  and policy  
661 loss  $\mathcal{L}_{\text{policy}}(\theta^{(t)}, \phi^{(t)})$ .  
662 9:     // — Confidence Module Update —  
663 10:    Update confidence module parameters  $\phi^{(t+1)}$  by minimizing meta-loss  $\mathcal{L}_{\text{meta}}(\phi^{(t)})$ .  
664 11:    // — Actual Policy Update —  
665 12:    Compute fresh confidence targets  $\hat{p}_n^{(t+1)} = V(I_n; \phi^{(t+1)})$  for samples in  $\mathcal{B}_{train}$ .  
666 13:    Update policy parameters  $\theta^{(t+1)}$  using  $\mathcal{B}_{train}$  with targets  $\hat{p}_n^{(t+1)}$  and policy loss  
667  $\mathcal{L}_{\text{policy}}(\theta^{(t)}, \phi^{(t+1)})$ .  
668 14: **end for**  
669 15: **return**  $\theta^{(T)}$ .

---

672 **B THEORETICAL ANALYSIS ON THE ALGORITHM**  
673674 **B.1 WEIGHTING SCHEME INTERPRETATION OF THE CONFIDENCE MODULE UPDATE**  
675

676 The parameters  $\phi$  of the confidence module  $V(\cdot; \phi)$  in MT-DPO are optimized via meta-learning.  
677 This process implicitly learns to assign an optimal target confidence  $p_n = V(I_n; \phi)$  for each prefer-  
678 ence pair  $(x, y_w, y_l)$  by adjusting  $\phi$  through its gradient updates.

679 The update of  $\phi$  is guided by the performance of a virtual policy  $\theta_{\text{virtual}}^{(t+1)}(\phi^{(t)})$  on the meta-dataset  
680  $\mathcal{B}_{meta}$ . The virtual policy is obtained by a one-step gradient descent of the main policy  $\theta^{(t)}$  on the  
681 policy loss  $\mathcal{L}_{\text{policy}}(\theta^{(t)}, \phi^{(t)})$ , which itself depends on  $p_n^{(t)}$ :

$$683 \theta_{\text{virtual}}^{(t+1)}(\phi^{(t)}) = \theta^{(t)} - \alpha \nabla_{\theta^{(t)}} \mathcal{L}_{\text{policy}}(\theta^{(t)}, \phi^{(t)}). \quad (12)$$

685 The confidence module parameters  $\phi$  are then updated as:

$$686 \phi^{(t+1)} = \phi^{(t)} - \eta \nabla_{\phi^{(t)}} \mathcal{L}_{\text{meta}}(\phi^{(t)}), \quad (13)$$

688 where  $\mathcal{L}_{\text{meta}}(\phi^{(t)}) = L_{\text{DPO}}(\pi_{\theta_{\text{virtual}}^{(t+1)}(\phi^{(t)})}; \pi_{ref})$  is evaluated on  $\mathcal{B}_{meta}$ .  
689

690 Applying the chain rule to  $\nabla_{\phi^{(t)}} \mathcal{L}_{\text{meta}}(\phi^{(t)})$  yields:

$$692 \nabla_{\phi^{(t)}} \mathcal{L}_{\text{meta}}(\phi^{(t)}) = \left( \frac{\partial \mathcal{L}_{\text{meta}}}{\partial \theta_{\text{virtual}}^{(t+1)}} \right)^T \frac{\partial \theta_{\text{virtual}}^{(t+1)}}{\partial \phi^{(t)}}. \quad (14)$$

695 Substituting  $\frac{\partial \theta_{\text{virtual}}^{(t+1)}}{\partial \phi^{(t)}} = -\alpha \nabla_{\theta^{(t)}, \phi^{(t)}}^2 \mathcal{L}_{\text{policy}}(\theta^{(t)}, \phi^{(t)})$ , the update direction for  $\phi$  is approximately  
696 proportional to:

$$698 \Delta \phi^{(t)} \propto \left( \nabla_{\theta_{\text{virtual}}^{(t+1)}} \mathcal{L}_{\text{meta}} \right)^T \left( \nabla_{\theta^{(t)}, \phi^{(t)}}^2 \mathcal{L}_{\text{policy}} \right). \quad (15)$$

700 The term  $\left( \nabla_{\theta_{\text{virtual}}^{(t+1)}} \mathcal{L}_{\text{meta}} \right)^T \left( \nabla_{\theta^{(t)}, \phi^{(t)}}^2 \mathcal{L}_{\text{policy}} \right)$  in Eq. 15 reflects the "alignment" between the change  
701 in policy learning direction—induced by adjusting target confidences  $p_n$  (controlled by  $\phi$ )—and the

desired direction for meta-objective optimization. If adjusting  $p_n$  steers the main policy’s learning direction closer to the optimal direction on  $B_{\text{meta}}$ , such an adjustment to  $\phi$  is reinforced. This mechanism enables  $V(\cdot; \phi)$  to adaptively generate  $p_n$ : for credibly correct preferences,  $p_n \rightarrow 1$  (reinforcing); for credibly incorrect preferences,  $p_n \rightarrow 0$  (correcting); and for ambiguous preferences,  $p_n \rightarrow 0.5$  (suppressing). This allows MT-DPO to dynamically adjust the influence of preference signals for more robust alignment.

## B.2 GENERALIZATION BOUND

We provide a generalization bound for MT-DPO, drawing inspiration Zhao et al. (2019). The theorem bounds the excess true risk of the empirically chosen confidence module parameters compared to the true optimal parameters.

**Theorem 1** *Let  $\theta \in \mathbb{B}^d$  be the parameter of MT-DPO in a  $d$ -dimensional unit ball. Let  $\mathbb{F}$  represent the underlying ground-truth distribution without label noise. Let  $m$  be the size of the meta data set. The generalization risk is defined as follows:*

$$R(\theta) = \mathbb{E}_{(x, y_1, y_2) \sim \mathcal{F}}[L_\theta(x, y_1, y_2)] \quad (16)$$

$$\hat{R}(\theta) = \frac{1}{m} \sum_{i=1}^m L_\theta(x_i, y_{1,i}, y_{2,i}) \quad (17)$$

where

$$L_\theta(x, y_1, y_2) := \ell_{\text{BCE}}(\hat{p}_\theta(x, y_1, y_2), p^*(x, y_1, y_2)) \quad (18)$$

Let  $\phi^* := \arg \max_{\phi \in \mathbb{B}^d} R(w^*(\phi))$  be the optimal coefficient vector in the unit ball, and  $\hat{\phi} := \arg \max_{\phi \in \mathcal{A}} \hat{R}(\theta^*(\phi))$  be the empirically optima among a candidate set  $\mathcal{A}$ , where  $\mathcal{A}$  is an  $\epsilon$ -cover in the Euclidean norm (i.e.  $\forall \phi \in \mathbb{B}^d, \exists \phi' \in \mathcal{A} : \|\phi - \phi'\| \leq \epsilon$ ).

Assume:

For each sample, the loss function is  $\sigma$ -sub-Gaussian with respect to the parameters  $\sigma$ .

The loss function is  $\lambda$ -Lipschitz continuous with respect to the parameters  $\phi$ :

$$|L_{\theta(\phi)} - L_{\theta(\phi')}| \leq \lambda \|\phi - \phi'\|.$$

For  $m$  sufficiently large, with probability at least  $1 - \delta$ :

$$R(\theta^*(\phi^*)) \leq \hat{R}(\theta^*(\hat{\phi})) + \frac{3\sigma\lambda}{\sqrt{m}} + \sqrt{\frac{d \ln(m)}{m} + \frac{2}{m} \ln\left(\frac{2}{\delta}\right)} \quad (19)$$

Theorem 1 bounds the excess risk for our MT-DPO approach, which leverages a meta-learned confidence module parameterized by  $\phi$ . It establishes that the true risk  $R(\hat{\phi})$  of the solution  $\hat{\phi}$  (obtained by minimizing empirical risk on the meta-dataset) approaches the optimal true risk  $R(\phi^*)$ , with this excess risk,  $R(\hat{\phi}) - R(\phi^*)$ , being bounded by terms on the order of  $O(\sqrt{d \ln(m)}/m)$ . The bound (Eq. 19) further indicates that this gap diminishes with an increasing meta-dataset size  $m$ . The term  $\sqrt{d \ln(m)}/m$  specifically highlights the trade-off: a higher dimensionality  $d$  of the confidence module parameters  $\phi$  (increased complexity) requires a larger meta-dataset  $m$  to maintain a similar generalization gap. Furthermore, the bound also underscores the influence of the sub-Gaussian nature of the loss ( $\sigma$ ) and its Lipschitz continuity ( $\lambda$ ) on the overall generalization performance. This provides theoretical support for the robustness and effectiveness of MT-DPO in learning adaptive confidence targets.

## C EXPERIMENTAL DETAILS

This section provides further details regarding the datasets, baseline configurations, and evaluation protocols used in our experiments, supplementing the information provided in Section ?? of the main paper.

756 C.1 DATASET DETAILS  
757758 Our experiments utilized two primary public preference datasets:  
759

760 • **Golden HH Dataset:** We used the official helpful training and test splits of the Golden  
761 HH dataset, which is derived from the Anthropic HH-RLHF dataset Bai et al. (2022a;b).  
762 The training split contains approximately 116K preference pairs, and the test split contains  
763 approximately 8.5K pairs. For specific details on the “Golden HH” variant if different from  
764 the standard HH-RLHF helpful split, please refer to Kong et al. (2024) Kong et al. (2024)  
765 from which we adapted some baseline comparisons.

766 • **OASST1 Dataset:** We used the standard training and test splits from the OpenAssistant  
767 Conversations (OASST1) dataset Köpf et al. (2023), as processed and utilized in prior DPO  
768 literature (e.g., Rafailov et al. (2023) for splits, Kong et al. (2024) for baseline numbers).  
769 The training split contains approximately 93K preference pairs, and the test split contains  
770 approximately 8.6K pairs after standard filtering.

771 **Data Processing:** For both datasets, prompts and responses were tokenized using the respective  
772 base LLM’s tokenizer (Llama-2 or Phi-2). Sequences were truncated or padded to a maximum  
773 length. For Golden HH, the maximum sequence length (prompt + response) was 1024 tokens. For  
774 OASST1, the maximum prompt length was 512 tokens and the maximum response length was 128  
775 tokens for each response.

776 **Meta-Dataset ( $\mathcal{D}_{meta}$ ) Construction:** As stated in the main text,  $\mathcal{D}_{meta}$  consisted of 150 clean  
777 preference pairs. These were randomly sampled without replacement from the original clean training  
778 split of each respective dataset (Golden HH and OASST1) *before* any synthetic noise injection.  
779 These 150 pairs were then excluded from the main training set  $\mathcal{D}_{train}$  used for policy optimization.

780 **Noisy Preference Simulation:** Symmetric label noise was introduced to  $\mathcal{D}_{train}$  (after excluding  
781  $\mathcal{D}_{meta}$ ) by randomly selecting a fraction  $\epsilon_{noise} \in \{0.1, 0.2, 0.3, 0.4\}$  of the preference pairs and  
782 swapping their  $y_w$  and  $y_l$  labels. The  $\epsilon_{noise} = 0\%$  condition corresponds to using the original clean  
783  $\mathcal{D}_{train}$ .

785 C.2 BASELINE CONFIGURATIONS  
786

787 The following provides specific configuration details for the baseline methods. All baselines used  
788 the same SFT model as their initial policy  $\theta^{(0)}$  and reference policy  $\pi_{ref}$  as MT-DPO. The DPO  
789 hyperparameter  $\beta$  was set to 0.1 for all DPO-based methods unless specified otherwise.

791 • **Vanilla DPO** Rafailov et al. (2023): Implemented following its original formulation  
792 (Eq. 2).

793 • **GDPO (Fixed  $\hat{p} = 0.75$ )** Furuta et al. (2024): The preference target probability  $\hat{p}$  was set  
794 to a fixed value of 0.75 for all training pairs in the cross-entropy loss formulation.

795 • **Conservative DPO (cDPO)** Mitchell (2023): Utilizes the cross-entropy loss (Eq. 5). For  
796 clean data ( $\epsilon_{noise} = 0\%$ ), the target  $\hat{p}$  was set to 1.0. For noisy data,  $\hat{p}$  was set to  $1 - \epsilon_{noise}$ ,  
797 assuming oracle knowledge of the true global noise rate.

798 • **Robust DPO (rDPO)** Liang et al. (2024): Implemented following the loss formulation  
799 described in their paper. Specific hyperparameters for rDPO (e.g.,  $\alpha_{rDPO}$ ,  $\gamma_{rDPO}$ ) were set  
800 to default values suggested by the original paper or tuned on a small held-out validation  
801 split (1K samples from  $\mathcal{D}_{train}$ ) if dataset-specific values were unavailable. Typical values  
802 were  $\alpha_{rDPO} = 0.5$ ,  $\gamma_{rDPO} = 0.5$ .

803 • **PerpCorrect-DPO** Kong et al. (2024): This involved a two-stage process:  
804 1. *Surrogate Model Training:* An auxiliary surrogate LLM (same architecture as the base  
805 SFT model) was trained on the clean meta-dataset  $\mathcal{D}_{meta}$  using DPO for 3 epochs with  
806 a learning rate of  $1 \times 10^{-5}$ .

807 2. *Data Denoising:* PPLDiff was computed for each pair in  $\mathcal{D}_{train}$  using this surrogate  
808 model. A PPLDiff threshold was determined by fitting two Gaussian distributions  
809 (one for presumed clean, one for presumed noisy based on initial PPLDiff quantiles)

810 to the PPLDiff values on  $\mathcal{D}_{train}$  and finding their intersection. Pairs identified as noisy  
 811 (PPLDiff suggesting the dispreferred response was better) had their labels flipped.  
 812

813 3. *DPO Training*: Vanilla DPO was then trained on this denoised version of  $\mathcal{D}_{train}$ .  
 814

### 815 C.3 EVALUATION PROTOCOL

816  
 817 The performance of aligned LLMs was evaluated by calculating their win rate against the initial SFT  
 818 model ( $\pi_{ref}$ ) on the respective test sets.  
 819

820 **LLM Judge and Prompt:** We employed GPT-4 (version ‘gpt-4-0613’) as our automated LLM  
 821 judge. For each prompt in the test set, responses from the evaluated model and the SFT baseline  
 822 were generated. These two responses were presented to GPT-4 in a randomized order using the  
 823 following prompt template:  
 824

825 You are an impartial AI assistant evaluating the quality of two anonymous responses (Re-  
 826 sponse A and Response B) to a given user prompt. Please consider helpfulness, harmlessness,  
 827 honesty, and overall quality.  
 828

829 User Prompt: [User Prompt Here]  
 830

831 Response A: [Response A Here]  
 832

833 Response B: [Response B Here]  
 834

835 Which response is better? (A) Response A is significantly better. (B) Response A is slightly  
 836 better. (C) Response B is significantly better. (D) Response B is slightly better. (E) Both  
 837 responses are of similar quality. (F) Both responses are very poor.  
 838

839 Please choose only one option (A, B, C, D, E, or F) and briefly explain your reasoning in  
 840 one or two sentences. Your choice (A-F):  
 841

842 **Win Rate Calculation and Tie Handling:** A response from the evaluated model was considered  
 843 a “win” if the judge selected (A) or (B) when the evaluated model’s response was A, or (C) or  
 844 (D) when it was B. Ties (option E) were counted as 0.5 wins for the evaluated model. Option (F)  
 845 responses, indicating both were very poor, were treated as ties for win rate calculation but noted for  
 846 qualitative assessment. To mitigate ordering bias, each pair was evaluated twice with the order of  
 847 Response A and Response B swapped, and the results were aggregated and averaged over the entire  
 848 test set.  
 849

### 850 C.4 STATISTICAL SIGNIFICANCE TESTING

851 As stated in Section 4.2.1, the win rate improvements of our implemented models, namely MT-DPO  
 852 and GDPO ( $\hat{p} = 0.75$ ), over our Supervised Fine-Tuned (SFT) baseline model were assessed for  
 853 statistical significance. This assessment was performed using the Wilcoxon signed-rank test. For  
 854 each test set and experimental condition (i.e., specific dataset, noise level, and base model), we  
 855 collected the paired outcomes (win, loss, or tie) of MT-DPO versus SFT, and GDPO versus SFT,  
 856 based on the LLM judge’s preference for each input prompt.  
 857

858 A win for the evaluated model (MT-DPO or GDPO) against the SFT baseline was coded as 1, a  
 859 loss as -1, and a tie as 0 for the purposes of the signed-rank test. We considered a p-value  $\leq 0.01$  to  
 860 indicate a statistically significant improvement over the SFT baseline. Across all conditions where  
 861 MT-DPO and GDPO demonstrated higher win rates than the SFT baseline as reported in Tables 1  
 862 and 2, these improvements were found to be statistically significant according to this criterion.  
 863

864 It is important to note that this statistical significance testing was confined to comparisons involving  
 865 models fully implemented and evaluated within our experimental framework against our SFT  
 866 baseline. Direct statistical comparisons (e.g., MT-DPO vs. Vanilla DPO where Vanilla DPO results  
 867 are adapted) involving baseline results adapted from Kong et al. (2024) Kong et al. (2024) were not  
 868 performed using the Wilcoxon signed-rank test, as the raw paired comparison data from their ex-  
 869 periments were not available to us. Discussions of performance differences involving such adapted  
 870 baseline results in the main paper are therefore based on the magnitude of observed differences in  
 871 the reported aggregate win rates.  
 872

864 

## D HYPERPARAMETER SETTINGS

865  
 866 This section details the hyperparameter settings used for MT-DPO and baseline models. Shared  
 867 hyperparameters (e.g., DPO  $\beta$ ) were kept consistent where applicable. Learning rates and batch  
 868 sizes were tuned based on preliminary experiments on a small validation set.  
 869

870 

### D.1 MT-DPO HYPERPARAMETERS

871 The key hyperparameters for MT-DPO are presented in Table 5. These were generally consistent  
 872 across both datasets for a given base model, with minor adjustments for optimal performance.  
 873

874 

Table 5: Hyperparameter settings for MT-DPO.

Hyperparameter	Llama-2-7B Value	Phi-2 Value
<b>Policy LLM (<math>\pi_\theta</math>)</b>		
Optimizer	AdamW	AdamW
Policy Learning Rate ( $\alpha$ )	$1 \times 10^{-6}$	$2 \times 10^{-6}$
Weight Decay (Policy)	0.01	0.01
$\mathcal{D}_{train}$ Batch Size ( $N_B$ )	8 (per GPU)	16 (per GPU)
DPO $\beta$	0.1	0.1
Gradient Clipping	1.0	1.0
Warmup Steps (Policy)	150	100
<b>Confidence Prediction Module (<math>V(\cdot; \phi)</math>)</b>		
Architecture	MLP: In(1) $\rightarrow$ FC(64,ReLU) $\rightarrow$ FC(1,Sigmoid)	Same
Optimizer	AdamW	AdamW
Confidence Module LR ( $\eta$ )	$2 \times 10^{-4}$	$3 \times 10^{-4}$
Weight Decay (Conf. Mod.)	0.0	0.0
$\mathcal{D}_{meta}$ Batch Size ( $M_B$ )	16 (per GPU, or matched $N_B$ )	16 (per GPU, or matched $N_B$ )
Input Feature $I_n$	Standardized PPLDiff	Standardized PPLDiff
<b>Training</b>		
Number of Epochs	1-2 (typically 1 for Golden HH, 2 for OASST1)	1-2 (typically 1 for Golden HH, 2 for OASST1)
SFT Model Training Epochs	1	1

891 The PPLDiff input to the confidence module was standardized (zero mean, unit variance) based on  
 892 statistics computed from an initial pass over a random 10% subset of  $\mathcal{D}_{train}$ .  
 893

894 

### D.2 BASELINE MODEL HYPERPARAMETERS

895 Hyperparameters for baseline models are detailed in Table 6. Policy LLM learning rates, DPO  $\beta$ ,  
 896 and batch sizes were kept consistent with MT-DPO’s policy LLM settings for the respective base  
 897 model (Llama-2-7B or Phi-2) to ensure fair comparison.  
 898

901 

Table 6: Key Hyperparameter settings for Baseline Models.

Baseline Method	Hyperparameter	Value (Llama-2-7B / Phi-2 where different)
<b>Vanilla DPO</b>	DPO $\beta$	0.1
	Learning Rate	Matched MT-DPO Policy LR (1e-6 / 2e-6)
<b>GDPO (Fixed <math>\hat{p}</math>)</b>	DPO $\beta$	0.1
	Learning Rate	Matched MT-DPO Policy LR (1e-6 / 2e-6)
	Fixed $\hat{p}$	0.75
<b>cDPO</b>	DPO $\beta$	0.1
	Learning Rate	Matched MT-DPO Policy LR (1e-6 / 2e-6)
	Target $\hat{p}$ (Noisy)	$1 - \epsilon_{noise}$ (Oracle)
<b>rDPO</b>	DPO $\beta$	0.1 (default, or tuned to 0.25 for some cases)
	Learning Rate	Matched MT-DPO Policy LR (1e-6 / 2e-6)
	$\alpha_{rDPO}$ , $\gamma_{rDPO}$	Typically 0.5, 0.5 (or tuned if performance was poor)
<b>PerpCorrect-DPO</b>	<i>Surrogate Model Training (DPO)</i>	
	DPO $\beta$	0.1
	Learning Rate	$1 \times 10^{-5}$
	Epochs on $\mathcal{D}_{meta}$	3-5 (typically 3)
	<i>Main DPO Training</i>	
	DPO $\beta$	0.1
	Learning Rate	Matched MT-DPO Policy LR (1e-6 / 2e-6)

918 D.3 COMPUTATIONAL RESOURCES  
919

920 All experiments were primarily conducted using NVIDIA A100 (80GB) GPUs. A typical training  
921 run for MT-DPO on the Golden HH dataset with the Llama-2-7B model for 1 epoch required approx-  
922 imately 15-20 hours on a single A100 GPU. Training Phi-2 models was generally faster, requiring  
923 approximately 8-12 hours for similar settings. The meta-learning step in MT-DPO introduces an  
924 overhead of approximately 15-20% per training step compared to vanilla DPO. Baseline models  
925 had similar or slightly shorter training times, with PerpCorrect-DPO incurring additional time (ap-  
926 prox. 1-2 hours) for surrogate model training on  $\mathcal{D}_{meta}$ . Distributed training using DeepSpeed  
927 ZeRO Stage 2 was employed when batch sizes exceeded single GPU memory capacity, particularly  
928 for Llama-2-7B. The total computational budget for all reported experiments, including SFT, DPO  
929 training runs, and evaluations, is estimated to be approximately 800-1200 GPU hours. We used  
930 PyTorch version 2.0, Hugging Face Transformers version 4.35, and TRL version 0.7.2.  
931

932 E FURTHER EXPERIMENTAL RESULTS  
933934 E.1 IMPACT OF THE ANCHOR MODEL ( $\pi_{anchor}$ ) ON MT-DPO PERFORMANCE  
935

936 The efficacy of MT-DPO, particularly its confidence prediction module, relies on the quality of the  
937 input signal, PPLDiff. The PPLDiff values are computed using an *anchor model*,  $\pi_{anchor}$ , as defined  
938 in Eq. 7. In our main experiments, we followed a standard practice Kong et al. (2024) and used the  
939 Supervised Fine-Tuned (SFT) model as the anchor model ( $\pi_{anchor} = \pi_{SFT}$ ). The rationale is that the  
940 SFT model has already been exposed to high-quality responses and thus provides a more domain-  
941 adapted and preference-aware baseline for perplexity calculation compared to the raw pre-trained  
942 model.

943 However, the choice of the anchor model is a critical design decision. A poorly performing or  
944 biased SFT model could potentially provide misleading PPLDiff signals, thereby degrading the per-  
945 formance of the meta-learning process. To investigate the sensitivity of MT-DPO to this choice, we  
946 conducted an additional experiment comparing the performance when using two different types of  
947 anchor models:

- 948 1. **SFT Model (as in main paper):** The Llama-2-7B model fine-tuned on the preferred re-  
949 sponses ( $y_w$ ) of the clean training data. This model serves as our default  $\pi_{anchor}$ .
- 950 2. **Base Pre-trained Model:** The original, off-the-shelf Llama-2-7B base model, without any  
951 supervised fine-tuning. This model has strong general language capabilities but no specific  
952 adaptation to the preference dataset’s domain or style.

953 **Experimental Design** We repeated the MT-DPO training runs on the Golden HH dataset with 20%  
954 and 40% symmetric label noise levels, using the Llama-2-7B architecture. All hyperparameters for  
955 the policy and confidence module training remained identical to those reported in Appendix D, with  
956 the only difference being the model used to compute PPLDiff for the confidence module’s input.  
957 The performance is measured by the win rate (%) against the SFT model, evaluated by GPT-4.  
958

959 **Results and Analysis** The results of this comparison are presented in Table 7.  
960

961 Table 7: Win Rates (%) of MT-DPO against SFT using different anchor models ( $\pi_{anchor}$ ) for PPLD-  
962 iff computation. Experiments were conducted on the Golden HH dataset with the Llama-2-7B  
963 model.

964 965 966 967 968 969 970 971 Anchor Model for PPLDiff	966 967 968 969 970 971 Noise Level ( $\epsilon_{noise}$ )	
	966 967 968 969 970 971 20%	966 967 968 969 970 971 40%
968 969 970 971 Base Pre-trained Model ( $\pi_{base}$ )	96.15	93.88
970 971 SFT Model ( $\pi_{SFT}$ ) – Default	<b>97.31</b>	<b>95.50</b>

972 The results clearly indicate that using the SFT model as the anchor model yields superior perfor-  
973 mance compared to using the base pre-trained model. With 20% noise, using  $\pi_{SFT}$  leads to a win

972 rate of 97.31%, a notable improvement over the 96.15% achieved with  $\pi_{base}$ . This gap widens under  
 973 a higher noise level of 40%, where the SFT-anchored model achieves 95.50% win rate, significantly  
 974 outperforming the base-anchored model's 93.88%.

975 We attribute this performance difference to several factors:

977

- 978 • **Domain Adaptation:** The SFT model is adapted to the specific style, topics, and vocabulary  
 979 of the Golden HH dataset. Its probability distributions are therefore more calibrated to  
 980 distinguish between in-domain high-quality versus low-quality responses, making the  
 981 resulting PPLDiff a more reliable signal for label consistency. The base model, lacking  
 982 this adaptation, may assign perplexities based on more general linguistic properties, which  
 983 might not correlate as strongly with the nuanced preferences in the data.
- 984 • **Preference Alignment Head-start:** The SFT process, by training on only preferred responses,  
 985 already nudges the model towards a distribution that favors desirable outputs. This  
 986 initial alignment makes it more sensitive to subtle flaws in dispreferred responses, leading  
 987 to a more discriminative PPLDiff signal.
- 988 • **Signal Stability:** A more informed anchor model likely produces a cleaner separation in  
 989 the PPLDiff distributions for correctly and incorrectly labeled pairs, which in turn makes  
 990 the meta-learning task for the confidence module easier and more effective.

991 In conclusion, while MT-DPO demonstrates robustness even with a non-domain-adapted base model  
 992 as the anchor, its performance is significantly enhanced when leveraging a more informed SFT  
 993 model. This highlights the importance of using a high-quality, relevant anchor model to generate the  
 994 most effective intrinsic signals for meta-learning adaptive confidence targets. This finding suggests  
 995 that investing in a good SFT model is a beneficial precursor not just for initializing the DPO policy,  
 996 but also for enabling more effective robust alignment methods like MT-DPO.

## 997 E.2 DETAILS ON LEARNED CONFIDENCE TARGET ANALYSIS

999 This section provides further context for the qualitative analysis of learned confidence targets pre-  
 1000 sented in Section 4.2.3.

1001 **Data for Analysis:** The data used for generating Figure 2 was a randomly selected subset of 5,000  
 1002 samples from the Golden HH training set after 30% symmetric label noise was applied. This subset  
 1003 included both instances whose original labels were preserved (and thus known to be "Clean Samples"  
 1004 with respect to the original annotation) and instances whose labels were intentionally flipped  
 1005 (thus known to be "Noisy (Flipped) Samples").

1006 **PPLDiff Calculation:** The PPLDiff values were computed using the SFT Llama-2-7B model as the  
 1007 anchor model  $\pi_{anchor}$ . Perplexity was calculated as  $\exp(-\frac{1}{L} \sum_{i=1}^L \log p(t_i | t_{<i}))$ , where  $L$  is the  
 1008 length of the concatenated sequence [prompt; response], and  $p(t_i | t_{<i})$  is the probability of token  
 1009  $t_i$  given preceding tokens, obtained from  $\pi_{anchor}$ . The PPLDiff was then  $\log \text{PPL}(\text{response}_1) - \log \text{PPL}(\text{response}_2)$ .

1010 **Confidence Module Output:** The  $\hat{p}_n$  values were obtained by passing the standardized PPLDiff of  
 1011 these 5,000 samples through the converged confidence module  $V(\cdot; \phi)$  of the MT-DPO model that  
 1012 was trained on the full noisy Golden HH dataset (Llama-2-7B,  $\epsilon_{noise} = 30\%$ ). The standardization  
 1013 of PPLDiff used the mean and standard deviation computed over the entire noisy training set.

1016 Observations from Figure 2 show that for PPLDiff values very close to zero (indicating high am-  
 1017 biguity or similar quality according to  $\pi_{anchor}$ ), the learned  $\hat{p}_n$  values tended to cluster around  
 1018 0.4-0.6, effectively down-weighting these uncertain samples in the policy update. The separation  
 1019 between the  $\hat{p}_n$  distributions for known clean and known flipped samples, while clear, exhibited a  
 1020 small overlap, indicating that PPLDiff is a strong but not perfect indicator of label correctness, and  
 1021 the confidence module learns to accommodate this imperfect signal.

## 1022 F QUALITATIVE CASE STUDIES

1023 To provide a more intuitive understanding of how MT-DPO operates, we present several case studies  
 1024 from the Golden HH dataset (trained with Llama-2-7B on 30% noise). These examples illustrate

1026 how the meta-learned confidence module assigns adaptive targets  $\hat{p}_n$  based on PPLDiff, and how  
 1027 this influences the final model's behavior compared to a vanilla DPO model trained on the same  
 1028 noisy data.

1029

1030 Table 8: Case Study 1: Successful Correction of a Mislabeled Preference.  
 10311032 **Prompt:** What are some fun things to do in San Francisco?1033 **Original Preference (Correct Label):**1034 **Chosen** ( $y_w$ ): San Francisco is a vibrant city! Some must-dos include visiting Alcatraz (book in advance!),  
 1035 walking across the Golden Gate Bridge, exploring Fisherman's Wharf, and riding a cable car. For something  
 1036 unique, check out the Mission District for amazing murals and burritos, or Golden Gate Park for its Japanese  
 1037 Tea Garden.

1038

**Rejected** ( $y_l$ ): Go to the bridge. See the prison. Eat fish.1039 **Noisy Preference in Training Data (Label Flipped):**1040 **Chosen**<sup>1</sup> ( $y_1$ ): Go to the bridge. See the prison. Eat fish.1041 **Rejected**<sup>1</sup> ( $y_2$ ): San Francisco is a vibrant city... (the detailed response)1042 **MT-DPO Analysis:**1043 **PPLDiff**( $y_1, y_2$ ): **+3.12** (The PPL of the short, unhelpful response is much higher)1044 **Learned Target**  $\hat{p}_n$ : **0.08** (Confidence module correctly identifies the label is likely wrong)1045 **Model Outputs:**1046 **Vanilla DPO (trained on noisy data):** You should go to San Francisco and see the bridge and the prison.  
 The wharf is also there.1047 **MT-DPO (Ours):** San Francisco offers many exciting activities! You could take a ferry to Alcatraz Island,  
 1048 walk or bike across the iconic Golden Gate Bridge, or explore the lively Fisherman's Wharf. For a more local  
 1049 experience, I'd recommend the colorful murals in the Mission District.

1050

1051 **Case 1: Successful Correction of a Mislabeled Preference** Table 8 showcases a typical example  
 1052 of a noisy label. The original, high-quality response was incorrectly labeled as "rejected" in the  
 1053 training data. The PPLDiff, computed by  $\pi_{SFT}$ , was strongly positive (+3.12) because the simplistic  
 1054 response is far less probable (i.e., has a higher perplexity) under a well-tuned language model than  
 1055 the detailed, helpful one. The confidence module, having learned this correlation from the meta-  
 1056 dataset, assigned a very low confidence target of  $\hat{p}_n = 0.08$ . This effectively reversed the gradient  
 1057 signal for this sample, treating the detailed response as preferred. As a result, the MT-DPO model  
 1058 provides a helpful, well-structured answer, while the vanilla DPO model, confused by such noisy  
 1059 signals, generates a simplistic and less helpful response.

1060

1061

1062

1063

1064

1065

1066

1067

1068

1069

1070

1071

1072

1073

1074

1075

1076

1077

1078

1079

1080 Table 9: Case Study 2: Handling Ambiguous Preferences.  
10811082 **Prompt:** Write a short poem about the moon.  
10831084 **Preference Pair in Training Data:**  
10851086 **Chosen** ( $y_1$ ): Silver orb in velvet night, / A silent watcher, soft and bright. / You pull the tides and guide the  
1087 way, / And turn the darkness into day.  
10881089 **Rejected** ( $y_2$ ): A lonely lantern in the sky, / Casting shadows from on high. / The poets dream, the lovers  
1090 swoon, / Beneath the magic of the moon.  
10911092 **MT-DPO Analysis:**  
10931094 **PPLDiff**( $y_1, y_2$ ): **-0.05** (Both poems are linguistically probable, PPLs are very close)  
10951096 **Learned Target**  $\hat{p}_n$ : **0.52** (Confidence module assigns a neutral target, down-weighting the instance)  
10971098 **Discussion:**  
10991100 This example illustrates a case of subjective preference or ambiguity. Both poems are well-written and on-  
1101 topic. The preference of  $y_1$  over  $y_2$  is weak at best. The anchor model reflects this by assigning very similar  
1102 perplexity scores, resulting in a PPLDiff close to zero. Consequently, MT-DPO’s confidence module learns to  
1103 output a target  $\hat{p}_n$  of 0.52, which is very close to 0.5. In the cross-entropy loss, this effectively down-weights  
1104 the contribution of this training instance, preventing the policy from strongly optimizing towards one specific  
1105 poetic style over another based on such a weak signal. This prevents overfitting to arbitrary stylistic preferences  
1106 present in the data. Vanilla DPO, in contrast, would treat this preference as absolute, potentially skewing the  
1107 model’s creative generation.  
11081109 Table 10: Case Study 3: A Limitation Case.  
11101111 **Prompt:** Explain the concept of quantum entanglement using an analogy.  
11121113 **Preference Pair in Training Data (Label Flipped):**  
11141115 **Chosen**’ ( $y_1$ ): It’s like having two coins that are linked. If you flip one and it’s heads, you instantly know  
1116 the other is tails, no matter how far apart they are. But it’s not that simple.  
11171118 **Rejected**’ ( $y_2$ ): Imagine you have a pair of “magic gloves.” You put them in two separate boxes and send  
1119 them to opposite ends of the universe. When you open your box and see a left-handed glove, you instantly  
1120 know the other box contains a right-handed glove. The state of one is intrinsically tied to the other, regardless  
1121 of distance. This is the essence of entanglement.  
11221123 **MT-DPO Analysis:**  
11241125 **PPLDiff**( $y_1, y_2$ ): **-0.21** (The simpler analogy was slightly more probable under the SFT model)  
11261127 **Learned Target**  $\hat{p}_n$ : **0.79** (Confidence module was misled by the PPLDiff signal)  
11281129 **Discussion of Limitation:**  
11301131 This example highlights a limitation of relying on PPLDiff. Here, a genuinely superior and more illustrative  
1132 analogy ( $y_2$ ) was mislabeled as rejected. However, the simpler, less precise analogy ( $y_1$ ) contained more  
1133 common phrasing and sentence structures, making it slightly more probable (lower perplexity) under our SFT  
1134 anchor model. This resulted in a small but negative PPLDiff. The confidence module, interpreting this as a  
1135 signal for a correct label, assigned a high confidence of  $\hat{p}_n = 0.79$ . In this case, MT-DPO was misled and  
1136 reinforced the incorrect preference. This illustrates that PPLDiff is a powerful heuristic but not an infallible oracle  
1137 for semantic correctness or quality, especially when comparing two fluent and topically relevant responses.  
1138 Improving MT-DPO’s robustness to such cases could involve incorporating more diverse signals into the  
1139 confidence module, a promising direction for future work.  
1140